ENHANCING PERFORMANCE OF ADDITIVELY MANUFACTURED AISI 316L BY ROTARY SWAGING

[1,2]Marek BENČ, [3]Karel DVOŘÁK, [1]Jiří DVOŘÁK, [1]Zdeněk JAKŮBEK, [2]Marek PAGÁČ

[1]*Institute of Physics of Materials, Academy of Sciences of the Czech Republic, Brno, Czech Republic, EU,*
marek.benc@vsb.cz
[2]*VSB-Technical University of Ostrava, Ostrava, Czech Republic, EU*
[3]*Brno University of Technology, Faculty of Civil Engineering, Czech Republic, EU*

Abstract

This work deals with the study of structure and physical properties of 316 L austenitic stainless steel prepared by additive manufacturing and subsequently processed by the technology of rotary swaging. The semi-finished products were printed on a Renishaw 3D printing machine using the SLM (Selective Laser Melting) method, during which the metal powder is gradually sintered via cladding of individual layers using a powerful laser. Subsequently, room temperature rotary swaging was applied to enhance the structure and properties of the SLM-manufactured semi-product. The structural analyses showed that the swaging process imparted significant refinement of the average grain size, which decreased down to approx. 1.3 μm (measured as the maximum feret diameter). As regards the physical properties, the density of the as-printed, as well as swaged, samples was measured using a pycnometer. As a result of forming, better material properties, such as increased density and improved hardness, were achieved. To confirm the advantages of the proposed approach consisting of a combination of 3D printing and deformation processing, all the results were compared with those acquired for an identical stainless steel prepared by conventional casting.

Keywords: 316L stainless steel, additive manufacturing (SLM), rotary swaging, density, microstructure

1. INTRODUCTION

Additive manufacturing (*AM*), or 3D printing, is among the alternative production methods that revolutionized the world of manufacturing. Additive processes are based on constructing three-dimensional parts by adding thin layers of material controlled by a digital CAD model [1]. During the selective laser melting (*SLM*) manufacturing process, a thin layer of powder is first applied to the substrate plate. Then the laser beam sinters the powder by which the connection to the base layer is created [2]. Despite many advantages of AM, including the ability to create complex geometries and functional prints and rapid production, problems arise especially when designing productions of small series of components. These problems include size limitations, surface roughness, low accuracy, and internal defects [1,3].

AM technologies can advantageously be combined with technologies of plastic deformation to improve the properties of the printed materials. Severe plastic deformation (SPD) methods can be used to homogenize the structures and eliminate residual porosity [4-6]. Nevertheless, SPD methods are limited to bulk samples with limited dimensions. On the other hand, rotary swaging (RS) is a process of intense plastic deformation, which is suitable for processing of large and long bulk workpieces [7,8]. During RS, the cross-sections of workpieces are gradually reduced, and their lengths increase [9]. The prevailing shear deformation mechanism is also favourable, as it supports elimination of residual porosity and structure refinement [10,11]. By combining the technologies of 3D printing and rotary swaging, improved mechanical properties can be achieved [12].

Stainless steel contains min. 12 wt% of Cr and typically consists of the austenitic phase. AISI 316L steel is one of the mostly used stainless steels due to its high strength, high corrosion resistance, and good formability. Therefore, this steel has various applications in the gas, automotive, and nuclear industries [13]. The aim of this work is to compare the structures and physical properties of AISI 316L stainless steel after printing and subsequent processing via cold rotary swaging. The results are compared with those acquired for an identical stainless steel prepared in a conventional manner.

2. MATERIAL AND METHOD

The semi-finished product for the experiment depicted in **Figure 1** was printed by the (*SLM*) method from 316L stainless steel powder (DIN 1.4404) on Renishaw AM400 3D printer. A blank in the shape of a cylinder with a height of 60 mm and a diameter of 25 mm was printed in the vertical direction from left to right using the meander printing strategy. The powder was melted by a 200 W laser, where each layer of new powder had a thickness of 50 μm. The printing took place in an inert atmosphere provided by argon gas with a gas purity of 99.998 %. The particle size of the powder was in the range of 15–45 μm. The chemical composition of the powder is given in **Table 1.**

Table 1 The chemical composition of the stainless-steel powders (wt%)

C	Si	Mn	P	S	N	Cr	Mo	Ni
< 0.03	1.00	2.00	0.045	0.030	0.11	16-18	2.0-3.0	10-14

Figure 1 The semi-finished product prepared by (*SLM)*

Figure 2 The bar processed by cold rotary swaging

The cold rotary swaging technology was chosen for the processing of the (SLM) semi-finished product from the original diameter of 25 to the final diameter of 10 mm. After rotary swaging, the rod (see **Figure 2**) was subjected to scanning electron microscopy (*SEM*) and specific gravity and hardness measurements. Structure observations were made using Tescan Lyra 3 FIB/SEM microscope at with the scanning step of 0.1 μm. Samples for microstructural analyses were manually ground on SiC papers and subsequently electropolished. Density was measured by the pycnometric method on samples with the size of 1x0.5 mm. Vickers hardness was measured on a ZwickRoell instrument. The hardness was measured on cross-sectional samples in the transverse direction with the load of 1000 g (HV 1), the indents were acquired with a distance of 1 mm from

each other. From these results, the average hardness was further calculated. This study presents the comparison of the results acquired for four individual material states marked as follows: 3D printed steel (*AP*), conventionally produced steel (*CP*), 3D printed after rotary swaging (*APS*), and conventionally prepared and processed by rotary swaging (*CPS*).

3. RESULTS AND DISCUSSION

3.1. Microstructure

The microstructures for all the investigated states are presented in (**Figures 3a** to **3d**). The average grain size (measured as the maximum feret diameter in μm) within the (*AP*) sample (**Figure 3a**) is 23.1 μm. The microstructure of the conveniently cast steel in the (**Figure 3b**) consists of smaller grains with the average size of 6.5 μm. In **Figures 3c** and **3d** are presented the microstructures of the steels processed by rotary swaging. After swaging, the average grain size is less than 2 μm. However, the microstructures of both the steels prepared by 3D printing and conventionally produced also contain several larger grains. Nevertheless, the relatively large fraction of low angle grain boundaries points to high development of substructure within these larger grains (see **Figure 3c**). The average grain size within the (*APS*) sample (**Figure 3c**) is 1.3 μm. Also microstructure of the conveniently cast steel after rotary swaging (*CPS*) in the figure (**Figure 3d**) consists of smaller grains with the average size 1.5 μm. Due to the large plastic deformation caused by the technology of rotary swaging, the grains were significantly refined.

a) After printing (*AP*)

b) Conventionally produced (*CP*)

c) Printed steel after rotary swaging (*APS*)

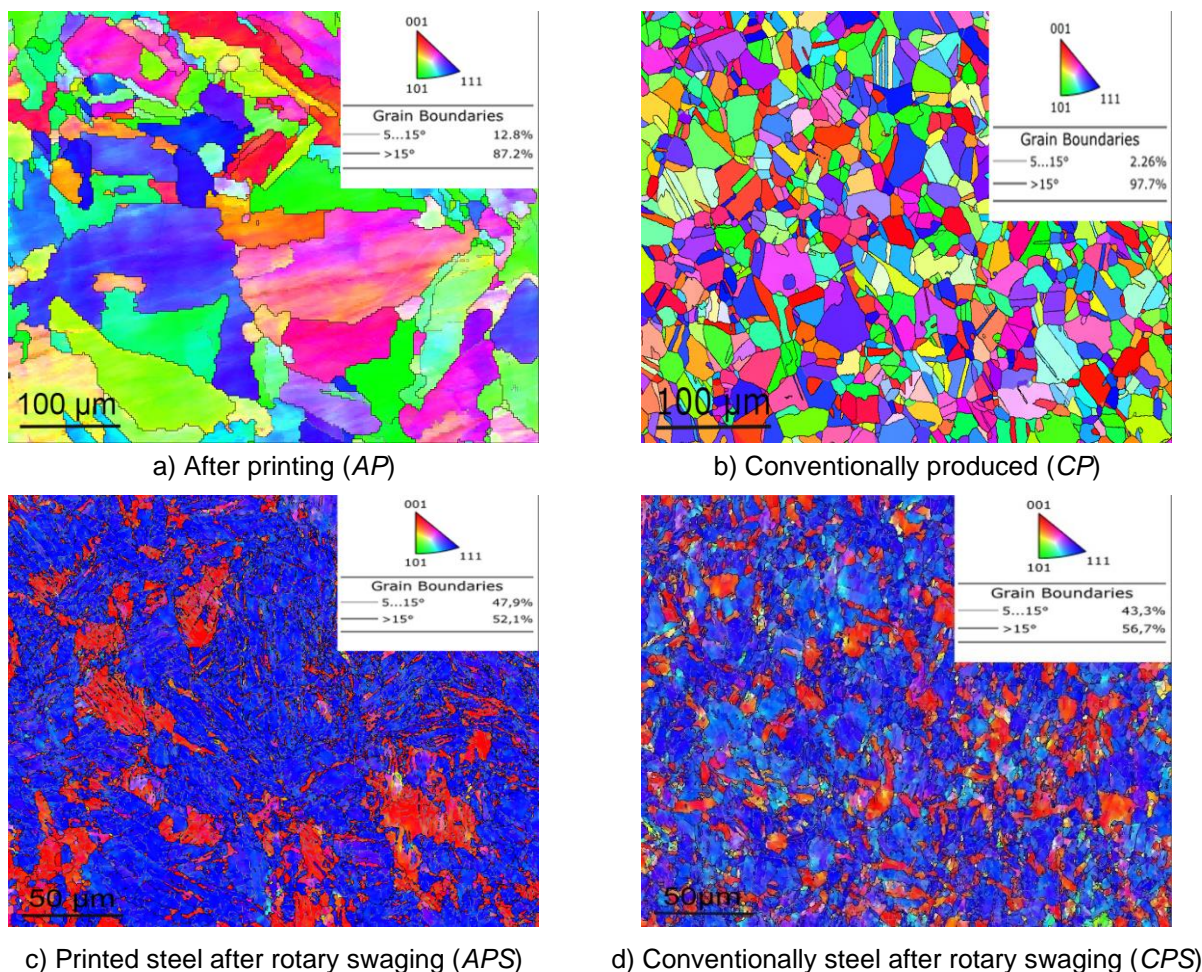d) Conventionally steel after rotary swaging (*CPS*)

Figure 3 Overview of microstructure for all processing methods

3.2. Density

The results of density measurements for all the examined samples are shown in **Figure 4** The first column depicts the average density for the (*AP* sample) – the measured value was 7.8405 g/cm³. A higher density of 7.9854 g/cm³ was measured for the conventionally produced steel (*CP* sample). After rotary swaging, the density increased to 7.9545 g/cm³ (*APS* sample), and to 8.0224 g/cm³ for the (*CPS* sample). As can be seen from the graph, the density increased due to the large plastic deformation imparted by the rotary swaging for both the material states, the as printed and conventionally cast.
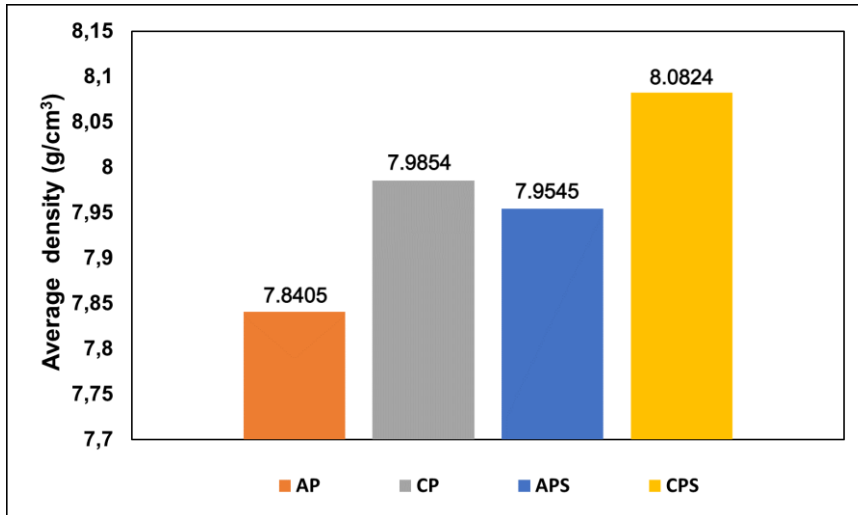

Figure 4 Results of average density measurements for investigated samples

3.3. Hardness

The average hardness from the individual states is presented **Figure 5.** The measured average hardness for the (*AP*) sample is 214 HV. The hardness measured for the (*CP*) steel sample shows comparable average HV value, i.e. 217 HV. In the case of the (*APS*) sample, the material was greatly strengthened and thus its HV increased to the value of 355 HV. Finally, the (*CPS*) sample exhibited the highest average microhardness of 358 HV. These results confirm the positive influence of the rotary swaging process on both the types of materials, i.e. as-printed as well as as-cast.
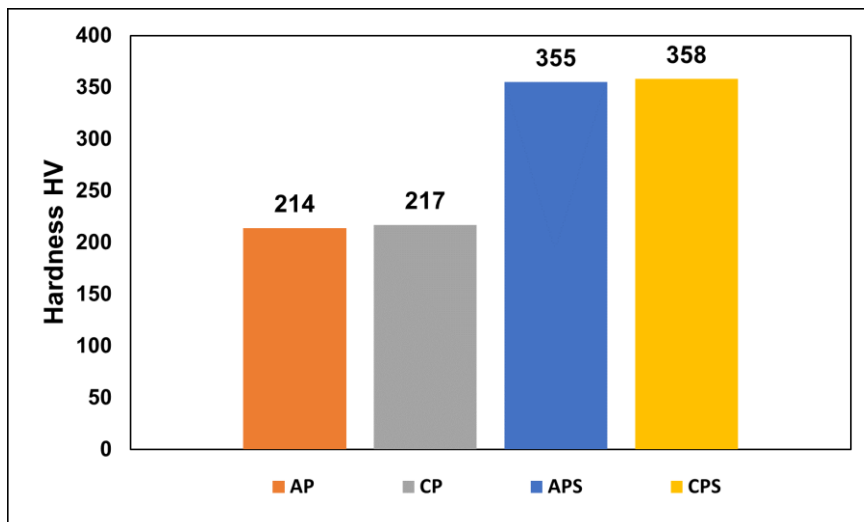

Figure 5 Measured average hardness results for all processing states

4. CONCLUSION

This work dealt with the observation of microstructures and physical properties of AISI 316L steel after 3D printing and subsequent processing via the cold rotary swaging technology. The data was further compared with experimental data acquired from conventionally cast and cold swaged AISI 316L bar. The results showed that the mechanical properties of the material improved significantly as the result of the cold rotary swaging. The microscopic analyses showed that, due to the large, imposed plastic deformation, the average grain size refined significantly from 23.1 μm (*AP*) to 1.3 μm (*APS*). From the density measurement results, it was found that the density after printing was 7.8405 g/cm^3. The cold rotary swaging then reduced the porosity and resulted in an increase in density to 7.9545 g/cm^3. Similar trend was observed also for the as-cast steel, the density of which increased from 7.9854 g/cm^3 to 8.0824 g/cm^3 after swaging. The positive influence of swaging was confirmed by the measurement of hardness, which documented improvement in the mechanical properties; from the original value of 214 HV after printing, the HV1 increased to 355 HV after swaging. Comparable increase was again observed for the conventional cast steel.

ACKNOWLEDGEMENTS

REFERENCES

[1] BRYTAN, Z., KRÓL, M., BENEDYK, M., PAKIELA, W., TANSKI, T., DAGNAV, M.J., SNOPINSKI, P., PAGÁČ, M., CZECH, A. Microstructural and Mechanical Properties of Novel Co-Free Maraging Steel M789 Prepared by Additive Manufacturing. *Materials. 2022*, vol. 15, pp.1734.

[2] SIMSON, T., EMMEL, A., DWARS, A., BOHM, J. Residual stress measurements on AISI 316L samples manufactured by selective laser melting. *Additive Manufacturing*. 2017, vol. 17, pp.183-189.

[3] ELLIOT, W., JOHN, C., ROBBINS, A., DAVID, G., SANDALA, C. Effects of spatial energy distribution-induced porosity on mechanical properties of laser powder bed fusion 316L stainless steel. *Additive Manufacturing*. 2021, vol. 39, pp. 101875.

[4] KUNČICKÁ, L., KOCICH, R., RYUKHTIN, V., CULLEN, J., LAVERY, N. Study of structure of naturally aged aluminium after twist channel angular pressing. *Materials Characterization*. 2019, vol. 52, pp. 94-100.

[5] KOCICH, R., KUNČICKÁ, L., MACHÁČKOVÁ, A. Twist Channel Multi-Angular Pressing (TCMAP) as a method for increasing the efficiency of SPD. *Materials Science and Engineering*. 2014, vol. 63, pp. 445-455.

[6] JAMILI, A., ZAREI-HANZAKI, A., ABEDI, H., MOSAYEBI, M., KOCICH, R., KUNČICKÁ, L. Development of fresh and fully recrystallized microstructures through friction stir processing of a rare earth bearing magnesium alloy. *Materials Science and Engineering*. 2020, vol. 775, pp.138837.

[7] KUNČICKÁ, L., KOCICH, R. Deformation behaviour of Cu-Al clad composites produced by rotary swaging. *Materials Science and Engineering*. 2018, vol. 369, pp. 10–13.

[8] KUNČICKÁ, L., MACHÁČKOVÁ, A., LAVERY, P., KOCICH, R., CULLEN, J., HLAVAČ, L. Effect of thermomechanical processing via rotary swaging on properties and residual stress within tungsten heavy alloy. *International Journal of Refractory Metals and Hard Materials*. 2020, vol. 87, pp. 105120.

[9] KOCICH, R., KUNČICKÁ, L., DOHNALÍK, D., MACHÁČKOVÁ, A., ŠOFER, M. Cold rotary swaging of a tungsten heavy alloy Numerical and experimental investigations. *International Journal of Refractory Metals and Hard Materials*. 2016, vol. 61, pp. 264-272.

[10] WANG, Z., CHEN, J., BESNARD, C., KUNČICKÁ, L., KOCICH, R., KORUNSKY, A. In situ neutron diffraction investigation of texture-dependent Shape Memory Effect in a near equiatomic NiTi alloy. *ActaMaterialia*. 2021, vol. 202, pp.135-148.

[11] STRUNZ, P., KUNČICKÁ, L., PŘEMYSL, B. Correlating Microstrain and Activated Slip Systems with Mechanical Properties within Rotary Swaged WNiCo Pseudoalloy. *Materials*. 2020, vol. 208, pp. 1996-1944.

[12] KOŘÍNEK, M., HALAMA, R., FOJTÍK, F., PAGÁČ, M., KRČEK, J., KRIZIKALLA, D., KOCICH, R., KUNČICKÁ, L. Monotonic Tension-Torsion Experiments and FE Modeling on Notched Specimens Produced by SLM Technology from SS316L. *Materials*. 2021, vol. 33, pp.1996-1944.

[13] SAEIDI, K., GAO, X., ZHONG, Y., SHEN, Z. Hardened austenite steel with columnar sub-grain structure formed by laser melting. *Materials Science and Engineering*. 2015, vol. 625, pp. 221-229.